*Macromol. Symp.* **79**, *31-44 (1994)*



# DIFFUSING-WAVE SPECTROSCOPY AND INTERFEROMETRY

David J. Pine*, D.A. Weitz, J.X. Zhu, and D.J. Durian

Exxon Corporate Research, Exxon Research & Engineering Company, Route 22 East, Annandale, New Jersey 08801, USA

A. Yodh and M. Kao

Department of Physics, University of Pennsylvania, Philadelphia, Pennsylvania 19104, USA

**Abstract**: Diffusing-wave spectroscopy and interferometry, the extensions of dynamic light scattering to materials which exhibit a very high degree of multiple scattering, have been used to measure the early-time, short length scale motion of Brownian particles. The transition from "ballistic" to "diffusive" motion is observed. In very dilute samples, this transition is described very well by theories which explicitly account for the time-dependent hydrodynamic interaction between a Brownian particle and the surrounding fluid. For particle volume fractions exceeding a few per cent, the data deviate from the theory for dilute suspensions, but exhibit a remarkable scaling with the suspension viscosity.

## INTRODUCTION

When a small particle, generally 5 nm to 10 μm in diameter, is suspended in a liquid, it executes rapidly fluctuating motions which are more or less random in space and time. This kind of movement, generally known as Brownian motion, arises from the random collisions of the particle with the surrounding liquid molecules and is typically described as a random walk. That is, the motion is characterized by a diffusion coefficient $D$ which linearly relates the mean square displacement of the particle to the time:

$$\left\langle \Delta r^2(t) \right\rangle = 6Dt. \tag{1}$$

For dilute suspensions of spherical particles, the diffusion coefficient is given by the Stokes-Einstein relation, $D = k_B T / (6\pi\eta a)$, where $k_B T$ is the thermal energy, $\eta$ is the viscosity of the liquid, and $a$ is the radius of the particle. While this expression for the mean square displacement is quite general, its validity cannot extend to arbitrarily short times. This can be readily demonstrated by calculating the particle velocity: since Eq. (1) implies that the root-mean-square displacement $\Delta r_{rms} \propto t^{1/2}$, the velocity $v \propto t^{-1/2}$. The velocity diverges at zero time. In fact, we expect the particle to move ballistically at very short times so that $\Delta r_{rms}$ should increase linearly in time. In this paper, we examine the physics of the crossover from the short-time ballistic motion to the diffusive motion of Brownian particles.

A simple analysis of Brownian motion was provided by Langevin many years ago. In this approach, the force acting on a Brownian particle in a liquid is divided into two parts, a slowly varying term, proportional to the particle velocity, which describes the viscous drag between the

 CCC 1022-1360/94/$ 04.00

particle and the liquid, and a rapidly varying term $f(t)$ which describes the effect of the random thermal collisions of the liquid molecules with the Brownian particle:

$$m\frac{dv}{dt} = -\zeta v + f(t). \tag{2}$$

Here, $m$ is the mass of the Brownian particle and $\zeta$ is the viscous drag which for dilute suspensions is given by $6\pi\eta a$. Solving this stochastic equation, one obtains,

$$\left\langle \Delta r^2(t) \right\rangle = 6D\left[t + \Im\left(e^{-t/\Im} - 1\right)\right], \tag{3}$$

where $\Im \equiv m/\zeta$. For early times $t << \Im$, Eq. (3) gives $\left\langle \Delta r^2(t) \right\rangle \cong (3k_BT/m)t^2$ in accordance with our expectations that the particle motion should be ballistic. For late times $t << \Im$, Eq. (3) gives $\left\langle \Delta r^2(t) \right\rangle \approx 6Dt$ as expected for diffusive motion. The crossover from ballistic to diffusive behavior occurs exponentially according to Eq. (3). Alternatively, this crossover can be seen via the velocity autocorrelation function obtained by taking the second derivative of Eq. (3),

$$\langle v(t)v(0) \rangle = \frac{k_BT}{m} e^{-t/\Im}, \tag{4}$$

which decays exponentially to zero. We will see that this simple analysis does not correctly describe Brownian motion at early times. Nevertheless, it does provide a convenient starting point from which to begin our discussion of the crossover from ballistic to diffusive particle motion.

In order to measure the crossover behavior, it is useful to determine approximately how far a Brownian particle moves in the time $\Im$ it takes the velocity autocorrelation function to decay appreciably. For a neutrally buoyant 1-μm-diameter sphere suspended in water, this distance is estimated to be

$$\Delta r \approx v\Im \approx \sqrt{\frac{3k_BT}{m}}\Im \approx 3\ \text{Å}. \tag{5}$$

Thus, we must be able to resolve the motion of a 1-μm-diameter sphere on a 3 Å length scale! The size of the particles suggests that dynamic light scattering (DLS) might be a suitable probe for these systems. However, conventional DLS using singly scattered light can accurately detect motion only on length scales roughly comparable to the wavelength of light and *longer*. By contrast, a relatively new technique, diffusing-wave spectroscopy (DWS), is able to resolve particle motion on over lengths scales of 1-100 Å. In the next section, we give a brief description of the salient features of diffusing-wave spectroscopy.

## DIFFUSING-WAVE SPECTROSCOPY

Diffusing-wave spectroscopy (DWS) is dynamic light scattering applied to systems that exhibit a very high degree of multiple scattering. In contrast to other schemes for working with multiply-scattered light, DWS does not seek to eliminate or minimize the effects of multiple scattering but instead directly analyzes the temporal fluctuations of highly multiply scattered light in order to extract information about the motion of the scatterers. By highly multiply scattered, we mean light that is typically scattered $10^2 - 10^7$ times. The essential point is that the transport of highly

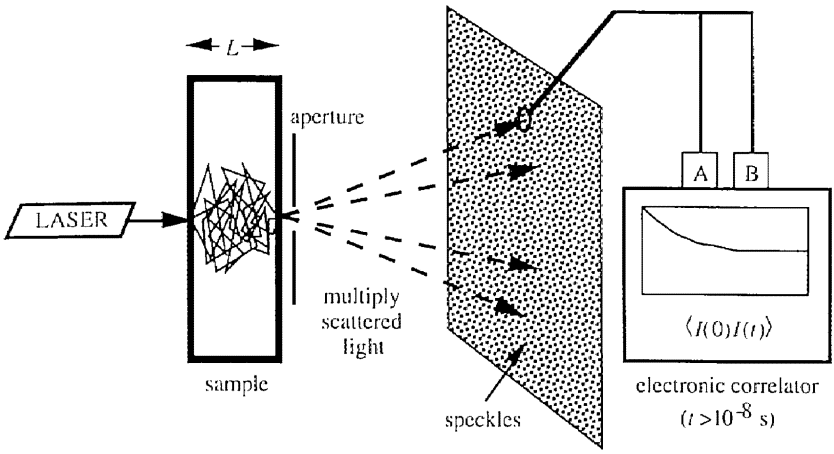


**Figure 1**: Schematic of DWS experiment. Laser light incident from the left on a rectangular glass cell is multiply scattered by the sample. Roughly one speckle of transmitted light is collected, split into two parts and detected by two photomultiplier tubes whose output is cross correlated by a fast electronic autocorrelator.

multiply scattered light can be described as a random walk, that is, by a diffusion equation for the photon energy density. This simplifying assumption allows us to adopt a statistical approach to our description of multiple scattering and eliminates many of the difficulties frequently associated with the analysis of multiple scattering.

A schematic illustration of a typical DWS experiment is shown in Figure 1. Light from a laser impinges on a sample contained in a rectangular glass cuvette which is approximately 1 cm wide and 1-5 mm thick. Transmitted light is collected from a small area ($\approx 0.02$ mm$^2$) on the other side of the cuvette directly opposite the point where the light entered. The sample, made up of roughly 1-μm-diameter polystyrene spheres suspended in water at 0.01-0.3 volume fraction, is optically dense so that essentially no unscattered light gets through the sample; the samples look like white paint or milk. Approximately one speckle of scattered light is collected, divided into two parts by a beam splitter, and sent to a pair of photomultiplier tubes whose output is cross correlated using a very fast (12.5 ns) correlator to obtain the intensity temporal autocorrelation function of the multiply scattered light. This cross-correlation scheme is needed to reduce dead time and afterpulsing effects.

The scattered electric field that is collected by the photomultiplier can be written as a sum over all possible paths $p$ that the photons take in traversing the sample,

$$\mathbf{E}(t) = \sum_p \mathbf{E}_p e^{i\phi_p(t)}, \tag{5}$$

where $\mathbf{E}_p$ is the amplitude and $\phi_p(t)$ is the phase of field from the $p^{th}$ path. The intensity of the scattered light is proportional to the square modulus of the scattered field:

$$I(t) \propto |E(t)|^2 = \sum_p \sum_{p'} \left(\mathbf{E}_p \cdot \mathbf{E}_{p'}\right) \exp\left[i\left(\phi_p(t) - \phi_{p'}(t)\right)\right]. \tag{6}$$

To a very good approximation, the fields from different paths are uncorrelated. When the particles in the sample move, the phase of the scattered light will fluctuate and, in turn, cause the intensity of scattered light to fluctuate in time. From Eq. (6), we see that the intensity of scattered light will be fully modulated, that is, it will go through one complete fluctuation, when the phase for a typical path changes by $\approx \pi$. This, of course, is the same condition that applies to singly scattered light in conventional DLS. The difference between DLS and DWS is that for DLS there is only one scatterer per path, and that scatterer must move a distance of roughly one wavelength or more in order to change the phase of the scattered light by $\pi$. By contrast, for DWS, there are many scatterers per path so that each particle must move only a small fraction of a wavelength in order for the phase on the entire path to change by $\pi$. Of course, some motions will tend to increase the path length and others will tend to decrease the path length, since the particle motions are essentially random. We can estimate the rms distance $\Delta r$ a typical particle moves in dephasing the light by noting that light executes a random walk. Thus, for a path consisting of $N$ scattering events,

$$\Delta r \propto \lambda / \sqrt{N}, \tag{7}$$

where $\lambda$ is the wavelength of light. Equation (7) is equivalent to saying that the total length of a typical path has changed by $\lambda$.

To obtain analytical expressions for the temporal autocorrelation function, one must exploit diffusive transport theory for light. While the theory and its application to DWS are straightforward, it is beyond the scope of this paper. The interested reader can refer to the literature for more details (Refs. 1-3). A useful, but simplified expression for the intensity temporal autocorrelation function for DWS in a transmission geometry (described above) is

$$g_2(t) \equiv \frac{\langle I(0)I(t)\rangle - \langle I\rangle^2}{\langle I\rangle^2} = \beta \left( \frac{\left(1 + \frac{4l^*}{3L}\right)x}{\left(1 + \left(\frac{2l^*}{3L}x\right)^2\right)\sinh x + \frac{4l^*}{3L}x\cosh x} \right)^2 \tag{8}$$

where

$$x = \frac{L}{l^*}\sqrt{k_0^2\left\langle \Delta r^2(t)\right\rangle}, \tag{9}$$

$L$ is the thickness of the sample, $l^*$ is the transport mean free path for the multiply scattered light, $k_0 = 2\pi/\lambda$, and $\beta$ is a numerical factor determined primarily by the light detection optics (Ref. 3). The transport mean free path is the length scale over which the direction of the multiply scattered light is randomized; that is, it is one random walk step length. A useful expression for $l^*$ is

$$l^* = \frac{1}{n\sigma\langle 1 - \cos\theta\rangle}, \tag{10}$$

where $n$ is the number density of scatterers, $\sigma$ is the total scattering cross section for a particle, and $\theta$ is the scattering angle. The transport mean free path can be calculated using Eq. (10) or it can be determined experimentally by measuring the transmission coefficient of the multiply scattered light in the sample.

Once $g_2(t)$ is measured and $l^*$ is determined, the experimental data can be inverted using Eqs. (8) and (9) to obtain an experimental measurement of $\langle \Delta r^2(t) \rangle$.

## DWS MEASUREMENTS FOR DILUTE SUSPENSIONS

Figure 2 shows a typical temporal autocorrelation function measured using DWS. The data shown were obtained from a sample of 1.53-μm-diameter polystyrene spheres suspended in water (Ref. 4). The correlation function was measured using an ALV-5000 correlator with a 12.5 ns minimum sample time. Figure 3 shows a measurement of the mean-square displacement obtained by inverting the data in Figure 2 using Eqs. (8) and (9). Note that the Brownian motion of a particle is resolved on lengths scales from as small as a few angstroms to approximately 100 Å. As expected, the mean square displacement approaches a slope of unity at the longest delay times measured. By contrast, the ballistic regime, where $\langle \Delta r^2(t) \rangle \approx t^2$, is not really probed in this measurement, even though the data span several decades in time over which the slope is significantly greater than one. This indicates that the transition from ballistic to diffusive behavior occurs much more slowly than expected from the simple Langevin theory presented in the Introduction.

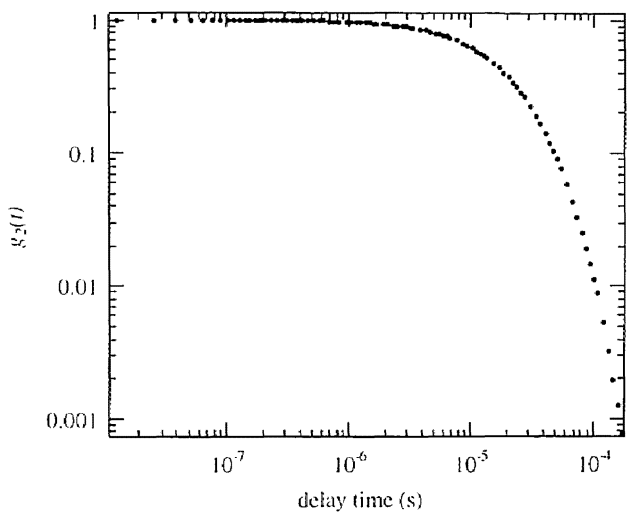


**Figure 2:** Typical temporal autocorrelation function measured using DWS.

In order to examine the transition to diffusive behavior in more detail, we define a time-dependent diffusion coefficient,

$$D(t) \equiv \frac{\langle \Delta r^2(t) \rangle}{6t}. \tag{11}$$

With this definition, $D(t)$ goes from zero at short times to a constant value equal to the short-time self diffusion coefficient $D_s$ at long times. By "long time," we mean times long enough to observe diffusive behavior but still considerably shorter than the time it takes a particle to diffuse a mean interparticle spacing; hence, the term "short-time" diffusion coefficient. In Figure 4, we plot $D(t)$ obtained from the data shown in Figure 3 and also the predicted behavior of $D(t)$ based on the solution to the Langevin theory given by Eq. (3). The simple Langevin theory does not describe the transition from ballistic to diffusive behavior observed in the data. The reason for this failure is the naïve treatment of the hydrodynamic friction between the fluid and the Brownian particle.

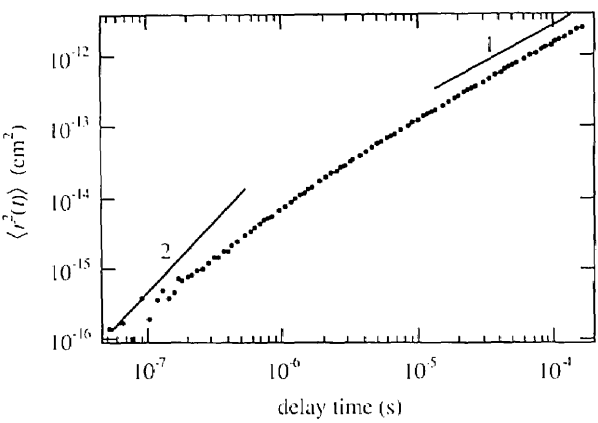


**Figure 3**: Mean-square displacement obtained by inverting the data in Figure 2 using Eqs. (8) and (9). The motion of a particle is resolved on lengths scales from a few angstroms to approximately 100 Å.

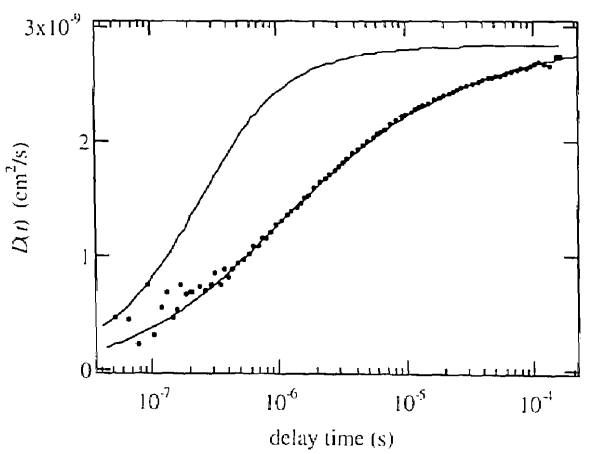


**Figure 4**: Time dependent diffusion coefficient obtained by dividing the data shown in Figure 3 by $6t$. The upper solid line is the predicted behavior of $D(t)$ based on the solution to the Langevin theory given by Eq. (3). The solid line through the data is the theoretical prediction of Hinch (Ref. 5).

The friction factor in the Langevin equation, Eq. (2), is assumed to be a constant; in dilute suspensions, its value is taken to be $\zeta = 6\pi\eta a$. However, this constant value is valid only for steady state drag where a particle is pulled through the fluid with a constant velocity and the fluid velocity field is time-independent (in the reference frame of the particle). The velocity of a Brownian particle, however, is constantly changing, as is the velocity field of the fluid in the vicinity of the particle. In this case, the friction factor is *time-dependent*. Thus, to obtain a proper description of the crossover from ballistic to diffusive behavior, the full time dependence of the fluid velocity field must be taken

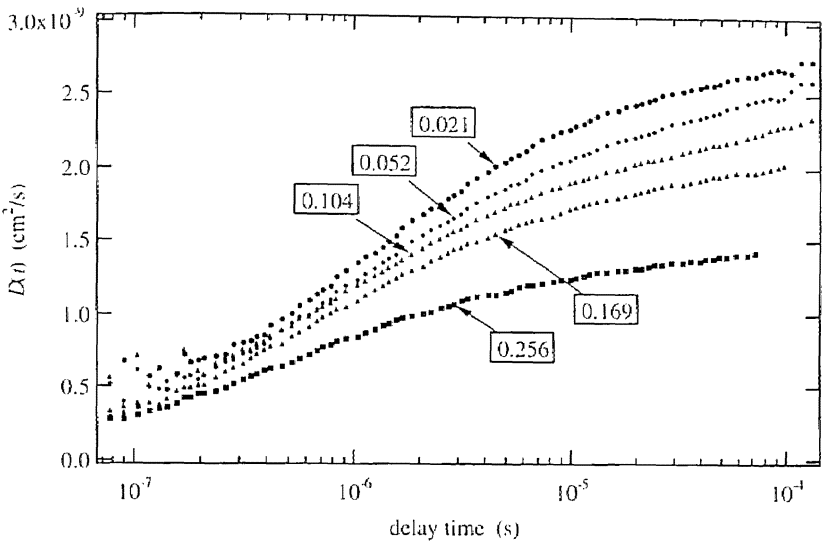


**Figure 5**: Time-dependent diffusion coefficient in concentrated suspensions.

into account. Such a procedure has been pursued first by Zwanzig and Bixon (Ref. 5), and later by Hinch (Ref. 6) and many others. They describe the fluid velocity field with the linearized Navier-Stokes equation which, for this situation, is essentially a diffusion equation for the fluid momentum with a diffusion coefficient equal to the kinematic viscosity, $\nu \equiv \eta / \rho$, where $\rho$ is the density of the fluid. Thus, the characteristic time for fluctuations in the particle and fluid velocities is $\tau_\nu = a^2 / \nu$. These fluctuations extend to very large distances, however, and propagate very slowly because of the diffusive nature of the hydrodynamics. As a consequence, velocity fluctuations die away very slowly; they decay asymptotically in time not exponentially as predicted in Eq. (4) by the simple Langevin theory, but as a power law,

$$\langle v(t)v(0)\rangle \propto t^{-3/2}. \tag{12}$$

Thus, the crossover from ballistic behavior occurs very gradually. In Figure 4, we show the prediction of the Hinch theory which incorporates a frequency-dependent (or equivalently, a time-dependent) friction coefficient which arises from a proper description of the coupling between the particle and the surrounding fluid. Since the density and viscosity of the fluid and the size and density of the particle are known, there are no adjustable parameters in the theory. The Hinch theory is in excellent agreement with our data. It is important to note that, while the expression for the velocity autocorrelation function in the Hinch theory is completely different from the simple Langevin result, the Stokes-Einstein expression for the diffusion coefficient remains valid.

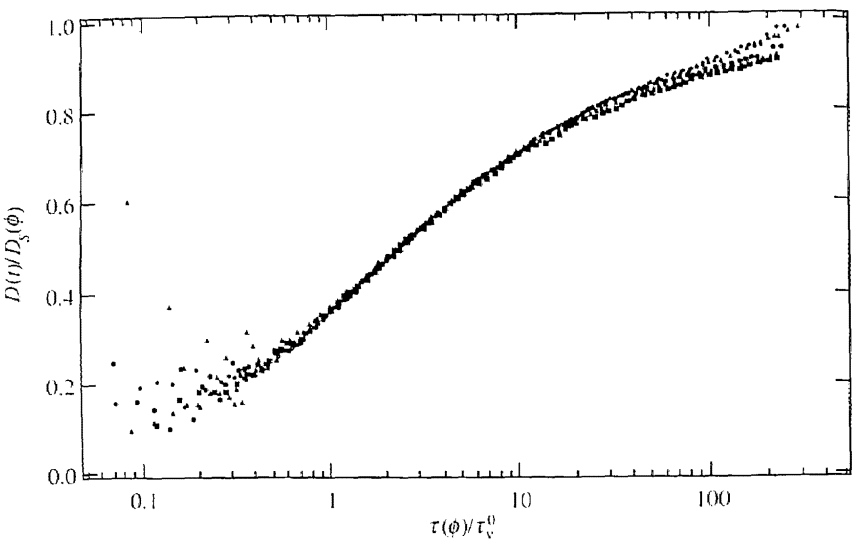


**Figure 6**: Scaling of $D(t)$: Time-dependent diffusion coefficient normalized by its asymptotic short-time self-diffusion coefficient vs a concentration-dependent scaled time. These are the same data shown in Figure 5.

## DWS MEASUREMENTS FOR CONCENTRATED SUSPENSIONS

We have also measured the time-dependent diffusion coefficient $D(\phi,t)$ in concentrated suspensions using DWS (Ref. 4). The results of these measurements are shown in Figure 5. The asymptotic values of $D(\phi,t)$ are in accord with Batchelor's theory for diffusion in concentrated suspensions and with the expectation that the self diffusion coefficient should decrease with increasing particle concentration (Ref. 7). Indeed, as concentration increases, $D(\phi,t)$ decreases over the entire time regime probed in our measurements. Physically, this decrease in $D(\phi,t)$ must arise because the flow around one particle is impeded by the presence of neighboring particles. Nevertheless, there is no theory available presently which can describe the time dependence of $D(\phi,t)$ in concentrated suspensions. In the absence of a detailed theory, one way to make progress is to look for scaling properties that the data may exhibit. One scaling scheme that seems to work well over the time scales probed in our experiments is to plot $D(\phi,t)/D_S(\phi)$ vs $\tau(\phi)/\tau_v$; that is, we plot the time-dependent diffusion coefficient normalized by its asymptotic short-time self-diffusion coefficient vs a concentration-dependent scaled time $\tau(\phi)/\tau_v$ in which $\tau(\phi)$ is adjusted for each concentration so as to obtain the best overlap of all the data. The results of this scaling are shown in Figure 6. The scaling is particularly good towards $1 \le \tau(\phi)/\tau_v \le 10$ where our data is most accurate. The spread in the data at the shortest times arises from very small uncertainties in $\beta$, the zero-time value of the temporal autocorrelation function. The spread in the data at the longest times arises from various small sources of noise, including laser intensity fluctuations, temperature drift, and electronic noise.

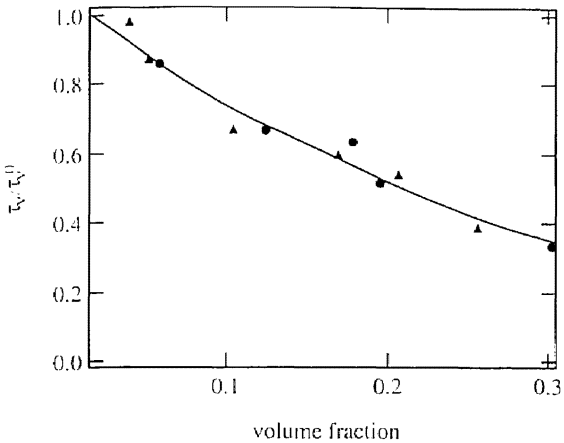


Figure 7: Reduced scaling time vs volume fraction for 1.53-μm-diameter and 3.09-μm-diameter spheres. The solid curve is the theoretical prediction of $\eta_0/\eta(\phi)$, the inverse high-frequency shear viscosity of the suspension normalized by its value at zero particle concentration.

In Figure 7, we plot the reduced scaling time $\tau(\phi)/\tau_\nu$ vs the volume fraction $\phi$. For comparison, we also plot the normalized reciprocal small-amplitude frequency-dependent viscosity $\eta_0/\eta(\phi)$ vs the volume fraction $\phi$. From these plots we see that the reduced scaling time follows the normalized reciprocal viscosity very closely. This suggests that a single Brownian particle is sensitive to the presence of the other Brownian particles and that their effect on the time-dependence of $D(\phi,t)$ is simply to modify the effective viscosity of the solution.

At the current time, there is no theoretical explanation for this apparent scaling of the data. Recently, Milner and Liu (Ref. 8) calculated the asymptotic long-time (or equivalently, the low frequency) behavior of $D(\phi,t)$ by considering two-particle hydrodynamic interactions; they found a different scaling of $D(\phi,t)$:

$$D(\phi,t) = D_s(\phi)\left[1 - \sqrt{4\,\tau(\phi)/(\pi t)}\right], \tag{13}$$

where $D_s(\phi)$ is the short time self diffusion coefficient calculated by Batchelor and

$$\tau(\phi) = \tau_\nu^0\left[1 - (15/4 - \delta\rho)\phi\right], \tag{14}$$

where $\delta\rho$ is the difference between the densities of the particle and the liquid (0.05 for polystyrene particles in water). The scaling we used corresponds to using Eq. (13) but with $\tau(\phi)$ defined as

$$\tau(\phi) = \tau_\nu^0\left[1 - 5/2\phi + O(\phi^2)\right]. \tag{15}$$

While Milner and Liu's result differs from the scaling we used, our data cannot distinguish between the two models for $t \geq 10\,\tau_\nu$. That is, Milner and Liu's theory provides a perfectly adequate description of our data for the range of time scales over which their theory is expected to apply.

It is also worth pointing out that the scaling we applied to our data in Figure 6 is not expected to apply to arbitrarily short time scales. Over sufficiently short time scales, there should not be enough time for neighboring particles to communicate with each other. An estimate of this time scale is the time it takes fluid momentum to diffuse between two particles, that is, $d^2/\nu$, where

$d$ is the distance between the surfaces of two particles separated by an average interparticle spacing. Thus, for times $t << d^2 / \nu$, we expect $D(\phi,t)$ to follow the single particle (infinite dilution) result for all particle concentrations. We estimate $d^2 / \nu$ to be 10-20 ns for our samples.

## DWI MEASUREMENTS FOR CONCENTRATED SUSPENSIONS

To investigate the potential breakdown of the scaling of $D(\phi,t)$ for times $t << d^2 / \nu$, we cannot use conventional electronic correlation techniques since the commercial correlators currently available do not go below 10 ns sample times. Indeed, a number of practical electronic problems make it very difficult to extend electronic correlators to significantly shorter time scales. To overcome this problem, we use a Michelson interferometer as an "optical correlator" (Ref. 9) Our apparatus is illustrated in Figure 8. As in the experiments described earlier, light from a laser is incident on a sample of thickness $L$. The transmitted light is chopped, sent into a Michelson interferometer, split (BS) and recombined, and then detected with a photomultiplier tube (PMT), whose output is measured with a lock-in amplifier. The field incident on the PMT is comprised of two parts, one from each arm of the interferometer. These two fields both come from the same area on the sample but are *time delayed* with respect to each other because of the different path lengths of the two arms; the time delay is simply the difference in the path lengths of the two arms divided by the speed of light, $t_2 - t_1 = 2(d_2 - d_1)/c$. Our apparatus measures the average intensity, proportional to the square of the electric field, incident on the PMT:

$$\begin{aligned} \langle I \rangle &\propto \left\langle \left| E(t_1) + E(t_2) \right|^2 \right\rangle \\ &= \left\langle \left| E(t_1) \right|^2 \right\rangle + \left\langle \left| E(t_2) \right|^2 \right\rangle + 2\left\langle E^*(t_1) E(t_2) \right\rangle \cos\left[\omega(t_2 - t_1)\right] \\ &= \tfrac{1}{2} I_{avg} \left[1 + g_1(t) \cos \omega t\right] \end{aligned} \tag{16}$$

where $t \equiv t_2 - t_1$ and $\omega$ is the angular frequency of the light. Note that $g_1(t)$, the electric field temporal autocorrelation function of the scattered light, appears as the amplitude of the interference fringes (i.e., the visibility) detected by the interferometer. The delay time is set by moving one of the mirrors; the maximum difference in path length for our interferometer is 6 m, which corresponds to a maximum delay time of $t = 20$ ns. The air wedge is used to make small changes in the relative optical path lengths in order to accurately measure the visibility at a given delay time.

In order to detect particle motion over the very short length scales we wish to probe, a typical photon passing through the sample must be scattered very many times. Thus, our samples must be very thick; a typical cell thickness for these experiments is 1-3 cm. Since the transport mean free path is about 40 μm (depending on the concentration of particles), the distance over which we can detect particle motion is $\Delta r \propto \lambda / \sqrt{N} \approx \lambda l^* / L \approx 0.5$ Å, where we have taken the number of random walk steps to be $N = \left(L / l^*\right)^2$. The distance a typical photon will travel through one of these samples is estimated to be $N l^* = \left(L / l^*\right)^2 l^* \approx 10$ m!

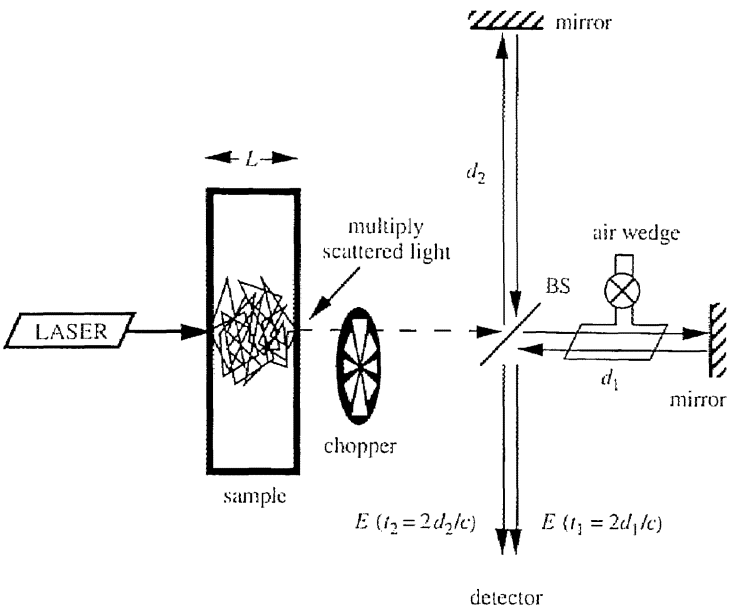


**Figure 8**: Michelson interferometer as an "optical correlator."

In Figure 9, we show typical interference fringes obtained at two different optical delays. The amplitudes of the fringes (i.e., the visibilities) at difference delay times are plotted in Figure 10. These measurements represent a direct measure of $g_1(t)$. Again, we can invert these data to obtain a measurement of $\langle \Delta r^2(t) \rangle$, which we plot in Figure 11 as the rms displacement vs time. At low volume fractions, we find excellent agreement between our data and the theory of Hinch. For reference, we also show the prediction of the simple Langevin theory which does not describe our data.

At higher volume fractions our data deviate from the Hinch prediction as shown in Figure 11. As the delay time increases, the rms displacement of the Brownian particle falls below that of the particle in dilute suspension. This is consistent with our expectation that hydrodynamic interactions with nearby particles will impede the motion of a given particle. We note, however, that the

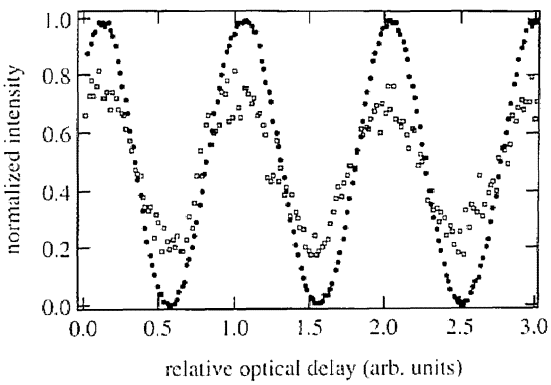


**Figure 9**: Typical interference fringes obtained at two different optical delays: 0 ns, closed circles; 20 ns, open squares.

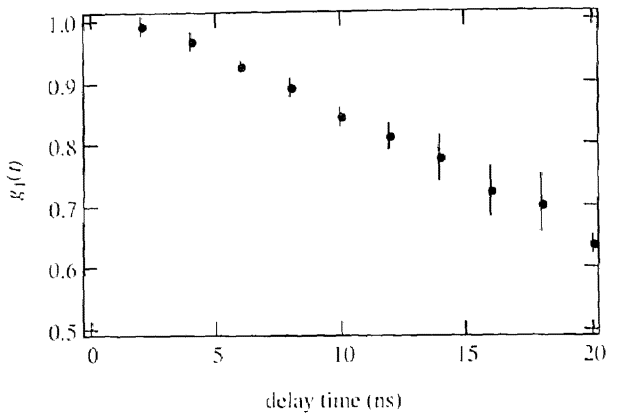


**Figure 10**: Amplitudes of the fringes (i.e., the visibilities) at difference delay times. These measurements represent a direct measure of $g_1(t)$.

characteristic time for fluid momentum to diffuse the mean distance $d$ between nearest neighbor particle surfaces is $d^2 / \nu \approx 12.5$ ns. We have observed these effects in all our concentrated samples ($\phi \leq 0.24$) on time scales significantly less than the time it takes the fluid momentum to diffuse the mean distance between nearest neighbor particle surfaces. The measurements suggest that average particle motion is still modified by hydrodynamic interactions, but that these interactions arise only occasionally between particles whose distance of closest approach is substantially smaller than the mean particle separation.

We also find that the data at short times scale the same way as do our data at longer time scales. This scaling is shown in Figure 12. However, we tested several other scaling schemes, such as

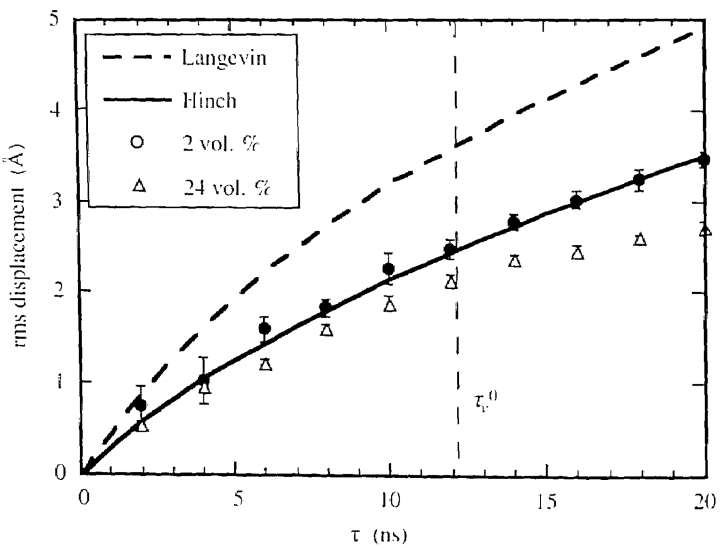


**Figure 11**: DWI measurement of the root means square displacement of a Brownian particle as a function of time. The data agree with the the Hinch prediction for the dilute sample but deviate from it at high volume fractions.

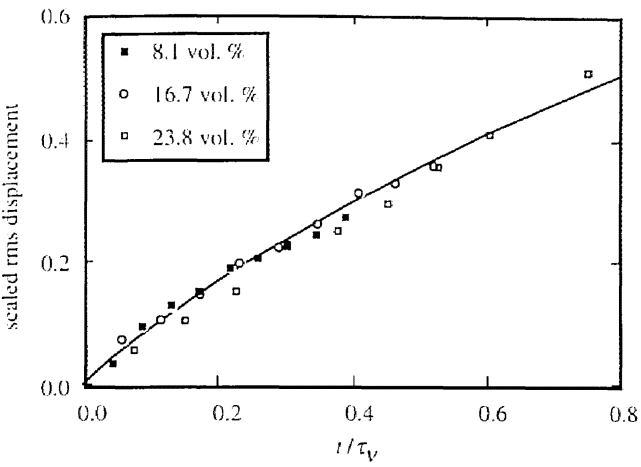


**Figure 12**: Scaling of the rms displacement at short times as measureed with DWI. The solid line is the scaled Hinch theory.

scaling both time and $D(\phi,t)$ by the inverse small amplitude viscosity, and these other schemes work equally well to the one shown in Figure 12. While it is beyond the scope of this paper, we also point out that because of the small size of our particles relative to the wavelength of light, our data *may* reflect some effects of collective motions of Brownian particles.

## CONCLUSIONS

In this paper we have shown how multiple light scattering techniques can be used to explore the very short time dynamics of Brownian particles. Such techniques should be applicable to any system which is optically opaque and does not exhibit too much absorption of light. In practice, this means that the system should have the appearance of milk; materials having a slightly gray or colored appearance should also be suitable for using these techniques. The time scales accessible with these DWS methods are (1) those time scales measurable by electronic correlators, which currently means times greater than a few tens of nanoseconds, and (2) times less than 20 ns using interferometric techniques, including not only the Michelson interferometer method used here but, in principle, also using Fabry-Perot interferometers.

## REFERENCES

(1) G. Maret and P. Wolf, *Z. Phys.* **B65**, 409 (1987).

(2) D.J. Pine, D.A. Weitz, P.M. Chaikin and E. Herbolzheimer, Phys. Rev. Lett. **60**, 1134 (1988). D.J. Pine, D.A. Weitz, J.X. Jhu and E. Herbolzheimer, J. Phys. France **51**, 2101 (1990).

(3) D.A. Weitz, D.J. Pine, in *Dynamic Light Scattering: The Method and Some Applications*, ed. W. Brown, Oxford University Press, 1993.

(4) J.X. Zhu, D.J. Durian, J. Müller, D.A. Weitz, and D.J. Pine, Phys. Rev. Lett. **68**, 2559 (1992).

(5) R. Zwanzig and M. Bixon, J. Fluid Mech. **69**, 21 (1975).

(6) E.J. Hinch, J. Fluid Mech. **72**, 499 (1975).

(7) G.K. Batchelor, J. Fluid Mech. **74**, 1 (1976), **131**, 155 (1983).

(8) S.T. Milner and A.J. Liu, to be published.

(9) M.H. Kao, A.G. Yodh, and D.J. Pine, Phys. Rev. Lett. **70**, 242 (1993).